Observation of $K=1/2$ octupole deformed bands in ^{227}Th

N. J. Hammond, G. D. Jones, P. A. Butler, and R. D. Humphreys
Oliver Lodge Laboratory, University of Liverpool, Liverpool L69 7ZE, United Kingdom

P. T. Greenlees, P. M. Jones, R. Julin, S. Juutinen, A. Keenan, H. Kettunen, P. Kuusiniemi, M. Leino, M. Muikku, P. Nieminen, P. Rahkila, and J. Uusitalo
Accelerator Laboratory, University of Jyväskylä, FIN-40351 Jyväskylä, Finland

S. V. Khlebnikov
V. G. Khlopin Radium Institute, 2nd Murinsky Prospekt 28, 194021 St Petersburg, Russian Federation
(Received 22 January 2002; published 4 June 2002)

High-spin states in ^{227}Th have been populated using the reaction ^{226}Ra$(\alpha,3n)^{227}$Th at a bombarding energy of 33 MeV. The high-spin rotational structures of this nucleus have been refined and extended. In addition, the linking of these structures with the low-spin states known from ^{231}U α decay has allowed a comprehensive decay scheme of this nucleus to be assembled for the first time. Four previously known rotational bands are interpreted as Coriolis coupled $K^{\pi}=1/2^{+}$ and $K^{\pi}=1/2^{-}$ bands, in agreement with predictions using a reflection-asymmetric mean field approach. The determination of decoupling parameters for these bands is consistent with the $a(K^{\pi}=1/2^{+})=-a(K^{\pi}=1/2^{-})$ rigid octupole rotor expectation. A further rotational band is interpreted as having $K^{\pi}=3/2^{-}$. Measured D_0/Q_0 ratios are consistent with an interpolation of the values given for neighboring even-even nuclei, providing further evidence for the significance of strong octupole correlations in this nucleus.

DOI: 10.1103/PhysRevC.65.064315 PACS number(s): 21.10.Re, 27.90.+b, 23.20.Lv

I. INTRODUCTION

The long standing prediction [1,2] of reflection asymmetric nuclei has been the subject of much experimental work over the last fifteen years. The susceptibility to this spontaneous reflection symmetry breaking effect arises from the proximity of (N,l,j) intruder orbitals and $(N-1,l-3,j-3)$ states. This condition is satisfied for N or $Z=34$, 56, 88, and 134, leading to the expectation of several nuclei that combine such proton and neutron numbers as candidates for the observation of reflection asymmetry. Indeed a large number of experimental evidences have shown the existence of regions around these candidate nuclei where the octupole interaction leads to reflection-asymmetric shapes (see Refs. [3,4] for a review of experimental and theoretical developments). The light actinides situated around $Z=88$ and $N=134$ have been experimentally shown to exhibit the largest octupole correlations. The possible coexistence of symmetric and reflection-asymmetric shapes in this region was first proposed by Chasman [5] who performed the earliest microscopic calculations on odd-A nuclei including octupole deformation. This study predicted the existence of such an effect in ^{227}Th. The calculations suggest that this coexistence of shapes should manifest itself in the observation of reflection-asymmetric orbitals with $K=1/2$ and symmetric orbitals with $K=3/2$. These states lie closest to the Fermi surface. More recently a reflection-asymmetric mean field approach by Ćwiok and Nazarewicz [6,7] has also predicted ^{227}Th to be one of the best candidates for the observation of such shape coexistence. One of the main spectroscopic fingerprints of reflection asymmetry in odd mass nuclei is the existence of parity doublets such as those observed in ^{223}Th [8] and ^{225}Th [9], and so this prediction would be supported experimentally by the existence of parity doublet structure for the $K=1/2$ bands and simple rotational structure for the $K=3/2$ bands. In the case of $K=1/2$ bands the Coriolis interaction leads to signature splitting and displaces intrinsic parity doublets. Within the framework of the particle-plus-rotor model the Coriolis signature splitting represents a partial decoupling of the single-particle motion from the rotating core. The *decoupling parameter a,* is a measure of the strength of this interaction and can be deduced from measured level energies. The most convenient method to identify reflection asymmetry in the spectroscopy of $K=1/2$ bands is, therefore, to determine decoupling parameters that follow the relationship $a(K^{\pi}=1/2^{+})=-a(K^{\pi}=1/2^{-})$ in the rigid octupole rotor limit.

Much work has been performed previously on ^{227}Th [10–14]. Low-energy states have been populated by the α decay of ^{231}U, the e^{-}-capture decay of ^{227}Pa and the β decay of ^{227}Ac. These studies allowed the determination of the ground state spin and speculated on the identification of several bandheads to which K values were assigned. The need to extend the known structure to higher spin led to a further experiment using the compound nucleus reaction ^{226}Ra$(\alpha,3n)^{227}$Th at 33 MeV with in-beam measurements of both γ- and e^{-}-decay by Manns *et al.* [14]. Although this study did identify many rotational bands to much higher angular momentum, it was not possible to convincingly correlate the high- and low-spin structures, hence no parities or spins were assigned to the unlinked rotational bands. We report here on the results of an investigation on ^{227}Th utilizing the same reaction and bombarding energy as Manns *et al.* The use of a more efficient Ge detector array has enabled us to collect in-beam γ-γ coincidence events with much greater statistics than previously observed. We have

TABLE I. Transition-energy lists used in the analysis of the γ-γ-γ coincidence matrix.

List	Description	Energies (keV)
A	Intraband transitions of band 1	162.0, 215.7, 263.7, 306.0, 342.7, 373.5, 396.7
B	Intraband transitions of band 2	119.1, 169.4, 223.7, 275.0, 321.0, 360.6, 394.5
C	Strong lines and x rays in ^{227}Th	64.8, 89.9, 93.1, 105.6, 169.4, 178.7, 211.2, 223.7, 265.7, 275.0, 303.7

been able to connect the previously known high- and low-spin structures in ^{227}Th and from the ensuing assignments of parity and spin to the rotational bands deduce a more comprehensive interpretation of this nucleus.

II. EXPERIMENTAL DETAILS AND RESULTS

A ^{226}Ra target was bombarded by a 33-MeV beam of α particles provided by the $K=130$ cyclotron at the University of Jyväskylä. The target consisted of a 250 μg/cm^2 thick $Ra(NO_3)_2$ layer, separated from other elements and daughter products and deposited upon a 30–40 μg/cm^2 Al backing. Prompt γ rays were detected in the Jurosphere array situated around the target position. The Jurosphere array consisted of 15 Eurogam Phase I [15], seven TESSA-type [16], and five NORDBALL-type [17] detectors with a total photopeak efficiency of 1.7% at 1.33 MeV. In total 1.6×10^8 γ deexcitations of fold 2 or above and 2.0×10^7 γ deexcitations of fold 3 or above were collected.

Demanding a fold of 3 or above was found to heavily reduce the unwanted background γ rays from the radioactive decay of the 12-μCi ^{226}Ra target. For this reason, all the spectra shown have been drawn from a γ-γ-γ cube, analyzed using the RADWARE package. This has enabled cleaner spectra to be produced at the expense of statistics. In cases where single gates have been set the resultant spectra are, therefore, the summed projections of coincidences on the two remaining axes. In some cases a list of transition energies has been used such that a projected spectrum consists of γ rays observed in coincidence with one or more members of the list. The transition-energy lists are given in Table I together with a brief description of their origin. Lists of all the γ-ray transitions assigned to ^{227}Th, which have been observed in our study are given in Tables II, III, and IV along with relative intensities. The two unconnected high-spin rotational structures observed are shown in Fig. 1. The six bands shown have all been observed previously by Manns *et al.* [14] and the same band labels have been used for ease of reference. Four of the rotational sequences have been extended to higher spin (see Figs. 2, 3, and 4 for the relevant spectra) and crucially, band 4 has been extended to lower spin due to the observation of the 105.2-keV and 126.5-keV transitions. The existence of the former is inferred from abnormal K_β x-ray intensities in several coincidence gates and from the presence

TABLE II. Measured properties of the intraband γ-ray transitions assigned to bands 1 and 2 including efficiency-corrected relative intensities. The γ-ray energies are estimated to be accurate to ±0.3 keV for the strong transitions ($I_\gamma>10$), rising to ±0.5 keV for the weaker transitions. I_{tot} and I_{e^-} have been calculated from I_γ using internal conversion coefficients taken from Ref. [27]. Except where otherwise specified, I_{tot}, I_γ, and I_{e^-} have estimated uncertainties of 15% for the strong transitions, rising to 20% for the weaker transitions. Doublet transitions, marked†, have associated uncertainties in intensity of 25%. In some cases the intensities could not be estimated without incurring even larger uncertainties and have, therefore, not been given. A prime example here is the 106.0 transition: This transition is masked by K_β x rays and 105.2-keV γ rays and proceeds by 90% internal conversion making γ ray intensities prone to a large error.

E_{tot} (keV)	I_{tot}	I_γ	I_{e^-}	Assignment	Band
106.0				$(13/2^+\rightarrow9/2^+)$	1
162.0	61.4	24.6	36.8	$(17/2^+\rightarrow13/2^+)$	1
215.7	50.2	33.2	17.0	$(21/2^+\rightarrow17/2^+)$	1
263.7	35.0	27.8	7.2	$(25/2^+\rightarrow21/2^+)$	1
306.0	15.8	13.6	2.2	$(29/2^+\rightarrow25/2^+)$	1
342.7	6.5	5.8	0.7	$(33/2^+\rightarrow29/2^+)$	1
373.5	2.0	1.8	<0.5	$(37/2^+\rightarrow33/2^+)$	1
396.7	0.7	0.6	<0.5	$(41/2^+\rightarrow37/2^+)$	1
412.6	<0.5	<0.5	<0.5	$(45/2^+\rightarrow41/2^+)$	1
119.1	100.0	15.7	84.3	$(9/2^-\rightarrow5/2^-)$	2
169.4†	79.8	35.3	44.5	$(13/2^-\rightarrow9/2^-)$	2
223.7†	64.6	44.6	20.0	$(17/2^-\rightarrow13/2^-)$	2
275.0	37.6	30.7	6.9	$(21/2^-\rightarrow17/2^-)$	2
321.0	17.7	15.5	2.2	$(25/2^-\rightarrow21/2^-)$	2
360.6	5.9	5.4	<0.5	$(29/2^-\rightarrow25/2^-)$	2
394.5	1.5	1.4	<0.5	$(33/2^-\rightarrow29/2^-)$	2
423.5	<0.5	<0.5	<0.5	$(37/2^-\rightarrow33/2^-)$	2

TABLE III. Same as Table II for the intraband transitions assigned to bands 3, 4, and 5.

E (keV)	I_{tot}	I_γ	I_{e^-}	Assignment	Band
224.5				$(23/2^-\rightarrow19/2^-)$	3
268.5	1.7	1.4	<0.5	$(27/2^-\rightarrow23/2^-)$	3
311.3	1.5	1.3	<0.5	$(31/2^-\rightarrow27/2^-)$	3
350.8				$(35/2^-\rightarrow31/2^-)$	3
385.8				$(39/2^-\rightarrow35/2^-)$	3
126.5	32.0	6.2	25.8	$(7/2^+\rightarrow3/2^+)$	4
178.7	25.7	12.7	13.0	$(11/2^+\rightarrow7/2^+)$	4
224.7†	21.6	15.0	6.6	$(15/2^+\rightarrow11/2^+)$	4
265.7	11.6	8.9	2.7	$(19/2^+\rightarrow15/2^+)$	4
303.7	5.6	4.8	0.8	$(23/2^+\rightarrow19/2^+)$	4
338.6	1.6	1.4	<0.5	$(27/2^+\rightarrow23/2^+)$	4
371.6	<0.5	<0.5	<0.5	$(31/2^+\rightarrow27/2^+)$	4
401.7	<0.5	<0.5	<0.5	$(35/2^+\rightarrow31/2^+)$	4
253.6	5.9	4.6	1.3	$(17/2^+\rightarrow13/2^+)$	5
297.6	3.0	2.6	<0.5	$(21/2^-\rightarrow17/2^-)$	5
334.4	1.2	1.1	<0.5	$(25/2^-\rightarrow21/2^-)$	5
364.9	<0.5	<0.5	<0.5	$(29/2^-\rightarrow25/2^-)$	5

TABLE IV. Same as Table II for interband transitions.

E (keV)	I_{tot}	I_γ	I_{e^-}	Assignment	Band
72.2	24.1	18.8	5.3	$(5/2^+\rightarrow 3/2^-)$	2→4
64.8	14.8	10.8	4.0	$(9/2^+\rightarrow 7/2^-)$	2→4
55.6				$(13/2^+\rightarrow 11/2^-)$	2→4
54.5				$(17/2^+\rightarrow 15/2^-)$	2→4
54.3				$(9/2^+\rightarrow 7/2^-)$	4→2
105.2				$(7/2^+\rightarrow)$	
113.9	30.8	22.5	8.3	$(11/2^+\rightarrow 9/2^-)$	4→2
169.2[†]	29.0	25.4	3.6	$(15/2^+\rightarrow 13/2^-)$	4→2
211.2	17.4	16.1	1.3	$(19/2^+\rightarrow 17/2^-)$	4→2
239.8	7.5	7.1	<0.5	$(23/2^+\rightarrow 21/2^-)$	4→2
257.4	3.2	3.0	<0.5	$(27/2^+\rightarrow 25/2^-)$	4→2
64.4	10.0	7.2	2.8	$(7/2^-\rightarrow 5/2^+)$	
190.6				$(15/2^-\rightarrow 13/2^+)$	3→1
209.4	5.9	5.4	<0.5	$(19/2^-\rightarrow 17/2^+)$	3→1
218.2	4.2	3.9	<0.5	$(23/2^-\rightarrow 21/2^+)$	3→1
223.0	1.2	1.1	<0.5	$(27/2^-\rightarrow 25/2^+)$	3→1
228.3	0.6	0.6	<0.5	$(31/2^-\rightarrow 29/2^+)$	3→1
236.4	<0.5	<0.5	<0.5	$(35/2^-\rightarrow 33/2^+)$	3→1
248.7	<0.5	<0.5	<0.5	$(39/2^-\rightarrow 37/2^+)$	3→1
233.7	10.9	10.2	0.7	$(13/2^-\rightarrow 11/2^+)$	5→4
262.6	9.6	9.1	<0.5	$(17/2^-\rightarrow 15/2^+)$	5→4
294.5	5.6	5.4	<0.5	$(21/2^-\rightarrow 19/2^+)$	5→4
325.2	0.9	0.9	<0.5	$(25/2^-\rightarrow 23/2^+)$	5→4
351.5	<0.5	<0.5	<0.5	$(29/2^-\rightarrow 27/2^+)$	5→4
253.5	1.3	1.2	<0.5	$(\rightarrow 17/2^-)$	6→5
269.7	0.6	0.6	<0.5	$(\rightarrow 21/2^-)$	6→5
279.9	<0.5	<0.5	<0.5	$(\rightarrow 25/2^-)$	6→5

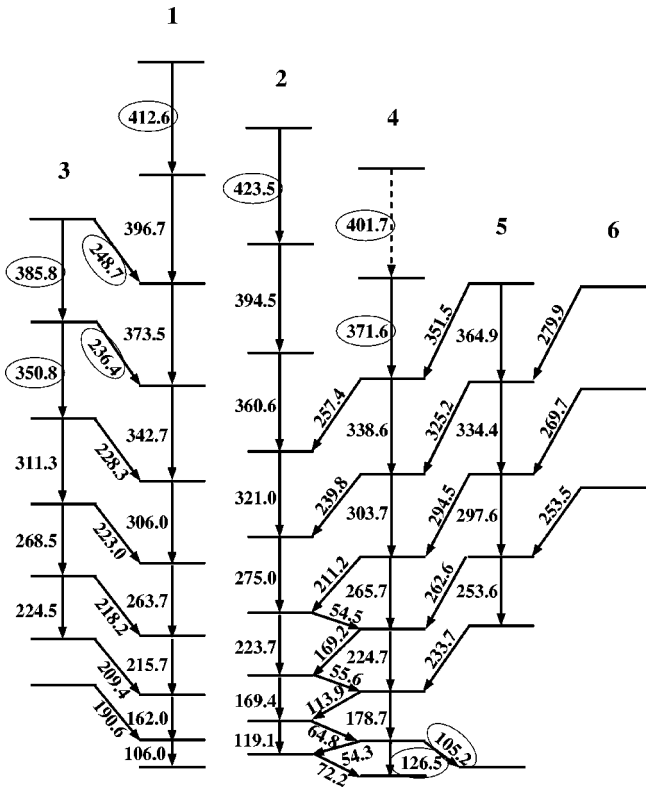

FIG. 1. Rotational bands in ^{227}Th observed in the ^{226}Ra$(\alpha,3n)^{227}$Th reaction at 33 MeV. The circled transitions are those which have not been previously observed. Dashed transitions represent tentative placements. The band number labels are referred to in the text.

of a 99.2-keV transition that was observed by Müller *et al.* [13] to decay from the level to which the 105.2-keV transition decays. It is impossible to determine the energy of the 105.2-keV transition conclusively due to the ubiquitous 105.6-keV thorium $K_{\beta 1}$ x rays and 104.8-keV thorium $K_{\beta 3}$ x rays, which incidentally also obscure the 106.0-keV transition. However, in Ref. [14], Manns *et al.* show e^--e^- coincidence spectra gated by the 162 L_{II} and 169 L_{II}, respectively, in both of which $E2$ transitions of ~106 keV are observed. While Manns *et al.* ascribe both of these coincidences to a single 106.0-keV transition, we note that the peaks appear to be at slightly different energies and we believe the latter to be the $E2$ transition to which we have assigned an energy of 105.2 keV. A reexamination of these spectra would be welcome in the light of the present decay scheme.

Gating cleanly upon the 126.5-keV transition is difficult as the line is strongly contaminated. For this reason a transition-energy list has been composed, which contains the energies of the three strongest thorium K x rays and also some of the ^{227}Th γ rays that are seen most prominently in the data. The energies contained in this list are displayed in Table I (list C). To ''clean up'' the 126.5-keV gate, γ rays are projected, which are observed in triple coincidence with a 126.5-keV γ ray and a member of the transition-energy list C. The resultant spectrum is displayed in Fig. 5.

Further differences exist between the scheme shown in Fig. 1 and that proposed by Manns *et al.* They proposed a 72.2-keV $E1$ transition depopulating the level in band 2 fed by 223.7-keV γ rays and feeding the level in band 1, which depopulates via 162.0-keV γ rays. In addition, a second $E1$ transition of 72.1 keV was observed, which was thought to feed out of the bottom of band 2. We have confirmed the placement of the latter transition, (favoring $E_\gamma=72.2$ keV rather than 72.1 keV), but we observe no evidence to support the existence of two transitions with this energy. The γ-ray spectrum measured in coincidence with the 72.2-keV transition is shown in Fig. 6 and clearly displays no peak at 162.0 keV. The 64.8-keV and 54.3-keV transitions were also proposed as links between bands 1 and 2 by Manns *et al.* These transitions are observed only weakly in the current data, predominantly due to the low efficiency of the Jurosphere array at such energies. However, the observation of a peak at 64.8 keV in the coincidence spectrum of Fig. 5 is in accordance with the scheme of Fig. 1. Moreover, the observations of Manns *et al.*, which led to the alternative placement, suggested coincidence between the 106.0-keV and 64.8-keV transitions, which can be explained through the introduction of the 105.2-keV transition. It should be noted that in general the coincidence spectra observed in the work of Manns *et al.* are more easily explained by two transitions around 105/106 keV as done in the present work. Spectra gated by 106-keV transitions are particularly difficult to reconcile if only a

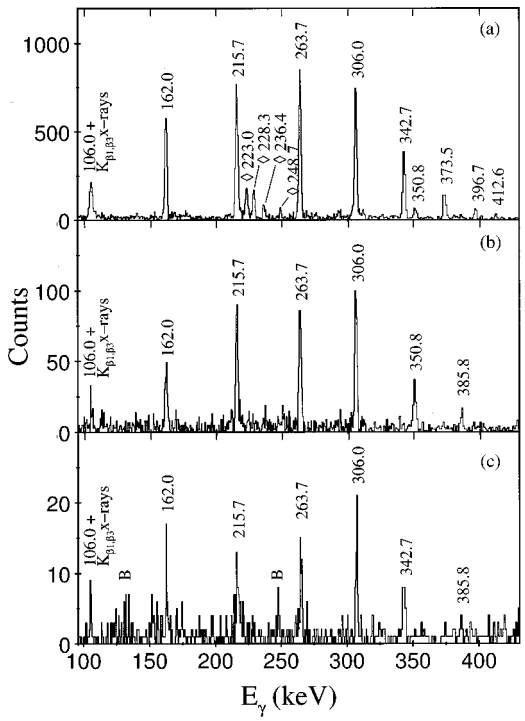

FIG. 2. γ spectra showing the evolution of bands 1 and 3 with increasing spin. (a) The projection of γ rays observed in coincidence with two or more further γ rays two of which must be members of the transition-energy list *A* (see Table I). (b) The projection of γ rays observed in coincidence with further two or more γ rays of which one must be a member of the transition-energy list *A* and another a 228.3-keV γ ray. (c) The projection of γ rays observed in coincidence with two or more further γ rays of which one must be a member of the transition-energy list *A* and another a 236.4-keV γ ray. The symbol ◊ is used to denote interband transitions and the label *B* denotes a background peak.

single 106-keV transition exists.

We should stress that in proposing the scheme of Fig. 1 we have assumed that the 178.7-keV transition has $E2$ character. Manns *et al.* assumed this transition to be $E1$ in nature based upon the strength of 178.7-keV γ rays and the absence of corresponding conversion electrons in e^- spectra gated by the 106.0-keV transition. However, the observed *M* and *N* conversion lines from the 162.0-keV transition mask the L_{II} and L_{III} conversion lines from the 178.7-keV transition and slight differences in gating conditions around 105.2–106.0 keV could strongly influence the relative intensity of 178.7-keV transitions observed by γ rays or conversion electrons. We, therefore, find no reason to assume $E1$ multipolarity for this transition and we favor an interpretation based upon $E2$ multipolarity. It will be seen that the assumption of $E2$ multipolarity for this transition (which is the exact energy sum of two cascade $E1$ transitions) allows the connection of the rotational structure to the low-lying levels; is consistent with the rotational spacings of band 4 and yields D_0/Q_0 ratios consistent with those for other $E1/E2$ branches in this nucleus.

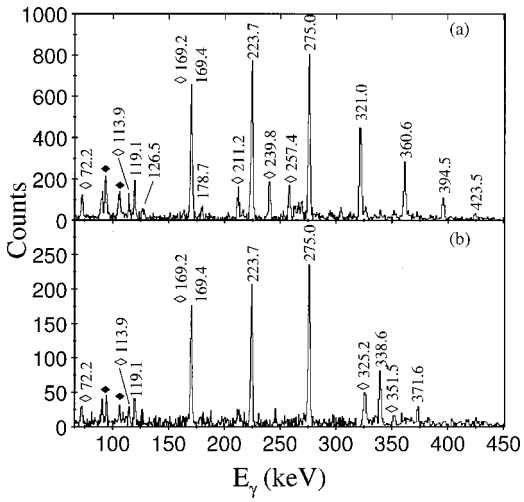

FIG. 3. γ-ray spectra showing band 2 and high-spin transitions in band 4. (a) The projection of γ rays observed in coincidence with two or more further γ rays two of which must be members of the transition-energy list *B* (see Table I). (b) The projection of γ rays observed in coincidence with two or more further γ rays of which one must be a member of the transition-energy list *B* and another a 239.8-keV γ ray. The symbols ◊ and ◆ are used to denote interband transitions and thorium *K* x rays, respectively.

III. DISCUSSION

A. Connecting high- and low-spin structures

The connection of the rotational levels to the low-lying states known from decay work is vital to assign spins and parities to these levels and to deduce an interpretation of this nucleus based upon all the available evidences. The low-lying intraband transitions in this nucleus, which have energies below 100 keV, proceed overwhelmingly by internal conversion, for example, a 76.5-keV $E2$ transition proceeds only 2% by γ-ray emission. Add to this the diminishing efficiency for γ-ray detection at such energies and it is clear that a connection of high- and low-spin structure is impossible based upon our observations alone. However, combining our observations with those of previous authors [13,14] suggests the structure displayed in Fig. 7. The lowest-lying thickly drawn levels shown in Fig. 7 are known from the α decay work of Müller *et al.* while the connection of the ro-

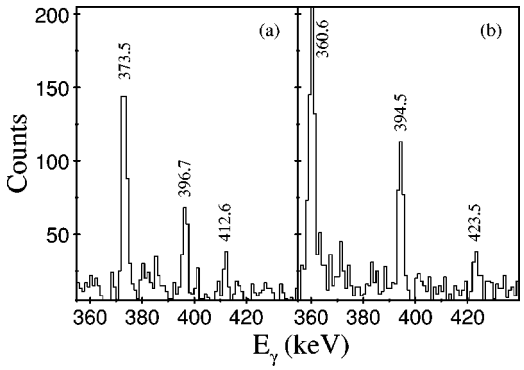

FIG. 4. Expanded scales of (a) Fig. 2(a) and (b) Fig. 3(a), showing the highest-spin transitions in bands 1 and 2.

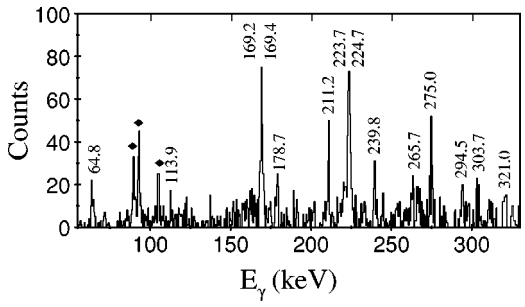

FIG. 5. Spectrum of γ rays observed in triple coincidence with two or more further γ rays of which one must be a member of the transition-energy list *C* (see Table I) and another a 126.5-keV γ ray. The symbol ♦ is used to denote thorium *K* x rays.

tational bands to these levels is based upon the evidence of our γ-γ-γ coincidences as well as the e^--e^- and e^--γ coincidences of Manns *et al.* The positioning of the 119.1-keV (band 2) transition is supported by the work of Manns *et al.* where conversion electrons from this transition were seen in coincidence with conversion electrons from the 76.5-keV and 68.6-keV transitions in addition to 72.1-keV and 64.4-keV γ rays. The position of the 119.1-keV transition leads directly to an energy difference between the $J^\pi=7/2^+$ and $J^\pi=3/2^+$ levels of 126.5 keV (refer to Fig. 7 for the spin and parity assignments, the unusual spin ordering will be discussed shortly). These levels are connected by the 126.5-keV (band 4) transition observed in our study, with the coincidence spectrum of Fig. 5 supporting such a placement. The 106.0-keV (band 1) transition has been previously observed [14] in coincidence with conversion electrons from a 66.9-keV transition and is, therefore, thought to feed the $J^\pi=9/2^+$ level as shown in Fig. 7. The 105.2-keV transition populates a level at 99.2 keV, which has been previously observed by Müller *et al.* As already noted, the 105.2-keV transition cannot be observed cleanly due to the presence of 105.6-keV thorium $K_{\beta1}$ x rays, 104.8-keV thorium $K_{\beta3}$ x rays, and in many cases 106.0-keV γ rays but this placement is consistent with the coincidence spectra observed. In addition to the 105.2-keV transition we have also shown in Fig. 7 the transition from the 99.2-keV level to the ground state. We have not shown all of the previously observed transitions from the 99.2-keV level to maintain clarity in Fig. 7 and we, therefore, refer the reader to the work of Müller *et al.* [13] for more details regarding this level. However, a 105.2-keV

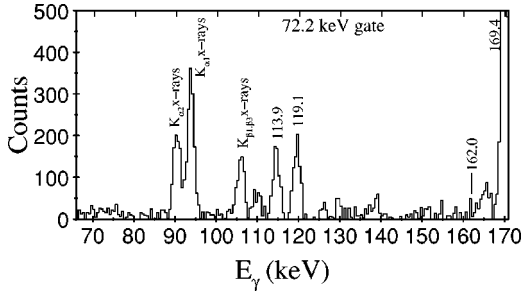

FIG. 6. Projection of γ rays in triple coincidence with γ rays of 72.2 keV. The absence of a 162.0-keV peak is indicated.

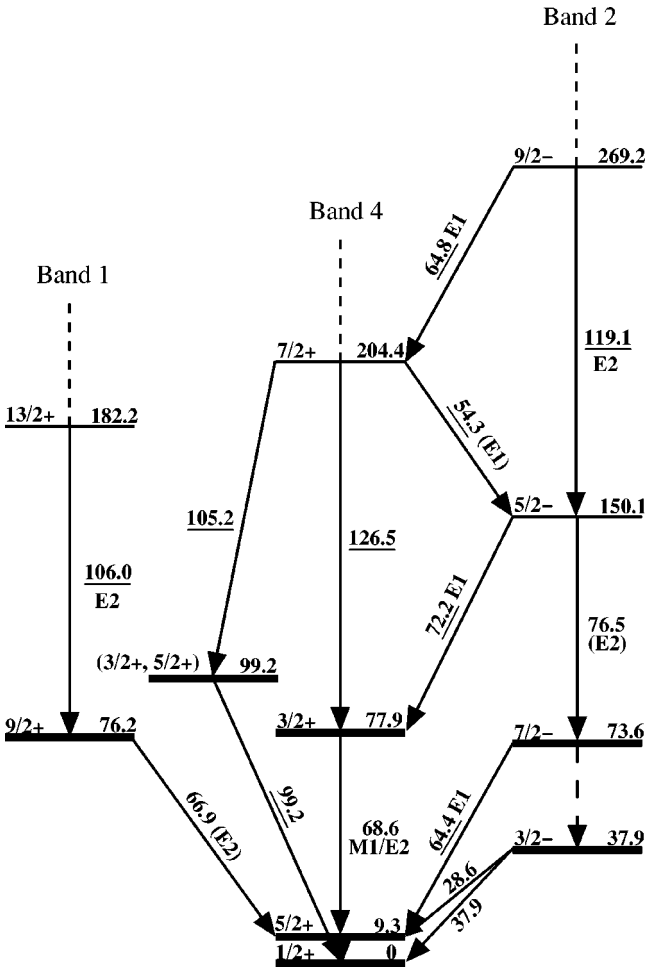

FIG. 7. The low-energy decay scheme. Levels shown in bold are known from decay studies and underlined transitions are those observed in the present study. The lowest $E2$ transitions of bands 1, 2, and 4 are shown connected to the low-lying structure. The band labels are shown to clarify the connection to high-spin structure and are not intended to label the low-spin sequences. This connection allows us the spin and parity assignments of almost all levels in the high-spin structure. The level at 99.2 keV possesses additional linking transitions to other low-lying levels that have not been drawn in the figure to avoid confusion; for a full description of these transitions see Ref. [13].

transition from the 204.4-keV ($7/2^+$) level imposes further restrictions on J^π for the 99.2-keV level in addition to those proposed by Müller *et al.* [13] and we, therefore, label the state as $3/2^+$ or $5/2^+$.

B. Interpretation of rotational bands

The connection of low- and high-spin structure discussed previously allows a full ^{227}Th level scheme to be constructed as shown in Fig. 8. The bands have been assigned *K* values and spin parity assignments have been made. The spin parity assignment of the ^{227}Th ground state has been the subject of much interest. Leander and Chen [18] first made the surprising suggestion that the ground state of ^{227}Th was $1/2^+$ in their seminal paper on odd $A=219-229$ nuclei. The first strong experimental evidence to support this assertion was

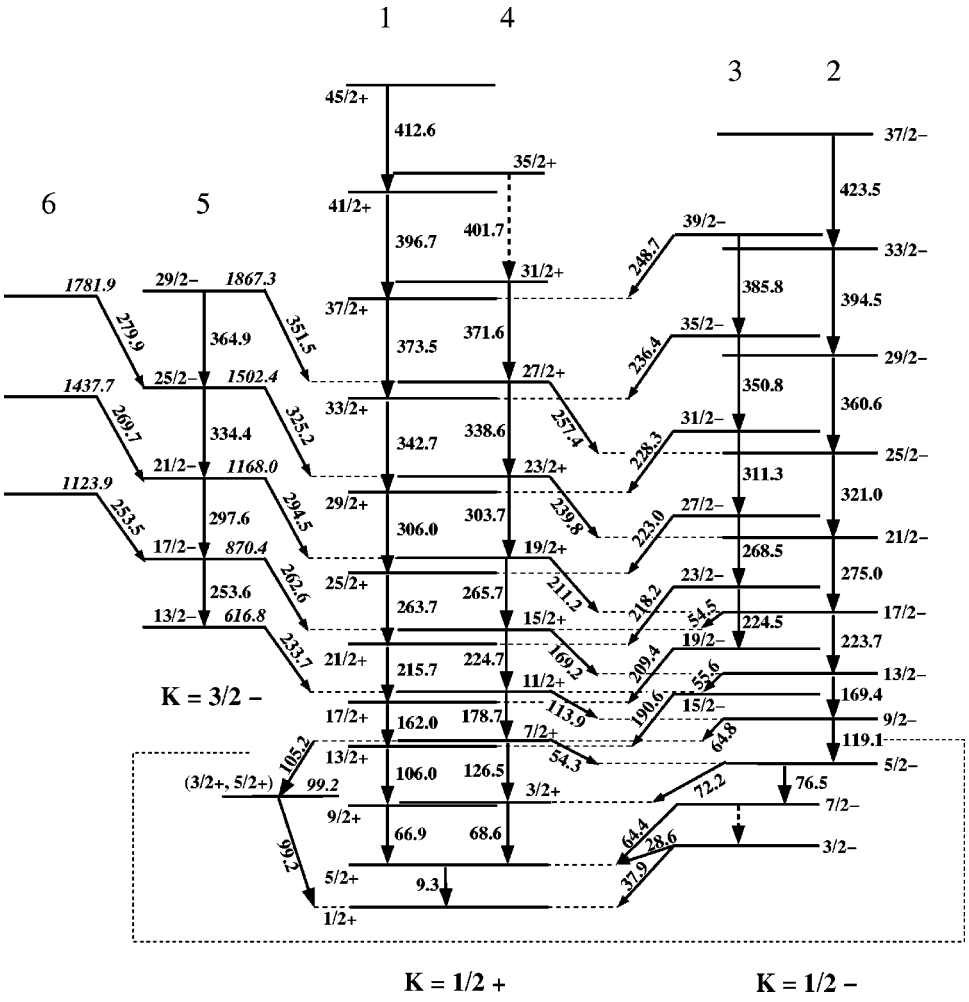

FIG. 8. The full level scheme of ^{227}Th. The $K^{\pi}=1/2^{\pm}$ parity doublet structure is emphasized. The band labels of Figs. 7 and 1 are shown at the top of the figure for ease of reference. Levels and transitions within the dashed box are not drawn to scale. Level excitation energies are shown for bands 5 and 6 and may be obtained for $K^{\pi}=1/2^{\pm}$ bands from Figs. 11 and 12.

the observation of maximum alignment for all (α,γ) angular correlations observed in the α decay of ^{227}Th into ^{223}Ra [19]. Low temperature nuclear orientation measurements [13] have subsequently strengthened this assignment. In Fig. 7 we have shown bands 1 and 4 to be extensions of the ground state band with positive parity determined from the $E2$ and $M1$ multipolarities ascertained by previous work [13,14]. These two sequences are, therefore, interpreted as the favored and unfavored signatures of a $K^{\pi}=1/2^{+}$ band. The assignment of spins to the $K^{\pi}=1/2^{+}$ band has been based upon the observed multipolarities while reproducing the spin ordering expected under the Coriolis perturbation (Fig. 10).

The level at 37.9 keV is known to have $J^{\pi}=3/2^{-}$ from the measured $E1$ decay to the ground state. For a $K^{\pi}=1/2^{-}$ band with $-1>a>-6$ the $J^{\pi}=3/2^{-}$ level has lowest excitation energy (Fig. 10) and the 37.9-keV level has thus been a strong candidate for a $K^{\pi}=1/2^{-}$ bandhead since this state was first identified [12]. Both this level and the $J^{\pi}=7/2^{-}$ level at 73.6 keV belong to the favored signature of the $K^{\pi}=1/2^{-}$ band with the expected $J^{\pi}=11/2^{-}$ member not observed. From the interpretation displayed in Fig. 7, the 119.1-keV transition feeds the $J^{\pi}=5/2^{-}$ level that is connected to the $J^{\pi}=7/2^{-}$ level via a 76.5-keV $E2$ transition. It is, therefore, likely that band 2 is the unfavored signature of the same $K^{\pi}=1/2^{-}$ band. Further support is provided by the spin assignments that give level ordering typical of a $K^{\pi}=1/2^{-}$ band. These assignments are based upon $E1$ transitions connecting this band to the unfavored signature of the $K^{\pi}=1/2^{+}$ band, which restrict the spins of many levels to one value only. In this way we have been able to confidently assign $J^{\pi}=5/2^{-}$ to the level at 150.1 keV in contrast to the $J^{\pi}=11/2^{-}$ assignment of Manns *et al.* We believe band 3 to be the high-spin extension of the favored signature of the $K^{\pi}=1/2^{-}$ band. The spin ordering is consistent with such an interpretation, as are the $E2$ intraband transition energies (varying slightly from those of the favored signature as in the $K^{\pi}=1/2^{+}$ case).

The angular momentum along the rotational axis J_x has been calculated for all sequences (except band 6) using

$$J_x(J)=\sqrt{(J+\tfrac{1}{2})^2-K^2}. \tag{1}$$

The rotational frequency dependence of J_x is shown in Fig. 9. The bands are labeled by parity and simplex with positive and negative simplex sequences given by

$$s=+i:\ \ J^{\pi}=\tfrac{1}{2}^{+},\tfrac{3}{2}^{-},\tfrac{5}{2}^{+},\tfrac{7}{2}^{-},\tfrac{9}{2}^{+},\ldots$$

$$s=-i:\ \ J^{\pi}=\tfrac{1}{2}^{-},\tfrac{3}{2}^{+},\tfrac{5}{2}^{-},\tfrac{7}{2}^{+},\tfrac{9}{2}^{-},\ldots$$

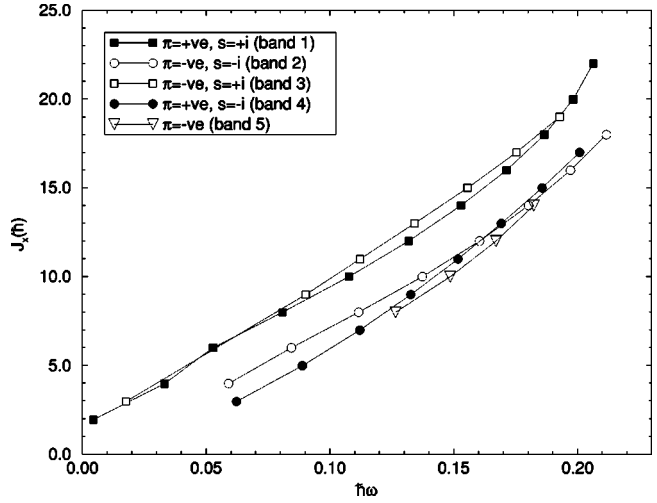

FIG. 9. A plot of angular momentum along the rotational axis as a function of rotational frequency. Sequences are labeled by simplex and parity with the rotational band labels also indicated for ease of reference.

The plots shown in Fig. 9 suggest that bands 1 and 3 as well as bands 2 and 4 do indeed form simplex partners with the gap between these two pairs of sequences being indicative of the signature splitting expected for $K^{\pi}=1/2^{\pm}$ bands.

We assign $E1$ multipolarity to the interband transitions between bands 5 and 4 based upon γ intensities and because transitions with $|K_1-K_2|>\lambda$ (where λ is the multipole order of the linking transition) are K forbidden, a $K^{\pi}=3/2^{-}$ interpretation seems likely for band 5. This band is also included in the alignment plot of Fig. 9. The interpretation of band 6 is difficult due to the paucity of information. This band is only tentatively proposed from weakly observed interband transitions to band 5. As the γ-ray intensities of these transitions do not conclusively indicate $E1$ multipolarity we choose not to attempt spin or parity labeling of the levels in band 6 and can, therefore, make no estimation of the K value of this band.

C. Extraction of decoupling parameters

The energy levels of a $K=1/2$ rotational band are given to second order by

$$E_{J,K}=\varepsilon_K-\frac{\hbar^2}{2\mathcal{J}}2K^2+\frac{\hbar^2}{2\mathcal{J}}\left[J(J+1)+\left(J+\frac{1}{2}\right)a(-1)^{[J+(1/2)]}\right]-B\left[J(J+1)+\left(J+\frac{1}{2}\right)a(-1)^{[J+(1/2)]}\right]^2, \quad (2)$$

where $[J+(1/2)]a(-1)^{[J+(1/2)]}$ is the Coriolis term and a is the decoupling parameter. The inverse moment of inertia $\hbar^2/2\mathcal{J}$ is often denoted as the energy parameter A as it corresponds to the inertial coefficient in the leading-order term. The second-order term, with the associated inertial parameter B, accounts for the rotation-vibration interaction and relaxes the dependence upon a constant moment of inertia throughout a given band. Equation (2) is plotted to first order in Fig. 10, the usual $J(J+1)$ relationship is seen on the y axis for $a=0$.

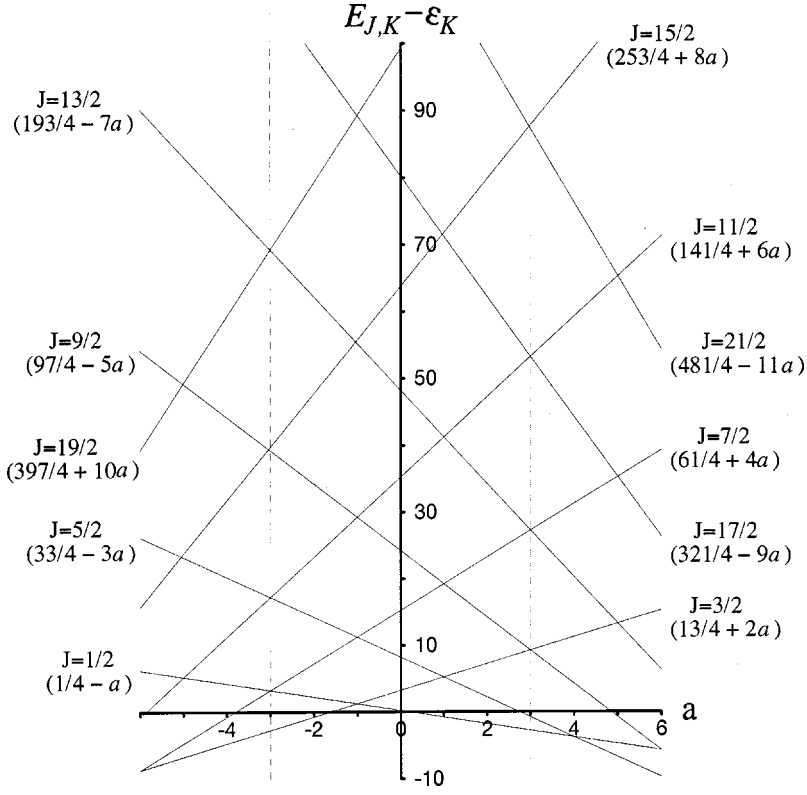

FIG. 10. Level energies in a $K=1/2$ band plotted against decoupling parameter a. The term in parentheses corresponds to the value of $[J(J+1)-2K^2+(J+1/2)a(-1)^{[J+(1/2)]}]$ [see Eq. (2)]. The vertical dashed lines represent the decoupling parameters predicted by Liang *et al.* as discussed in the text.

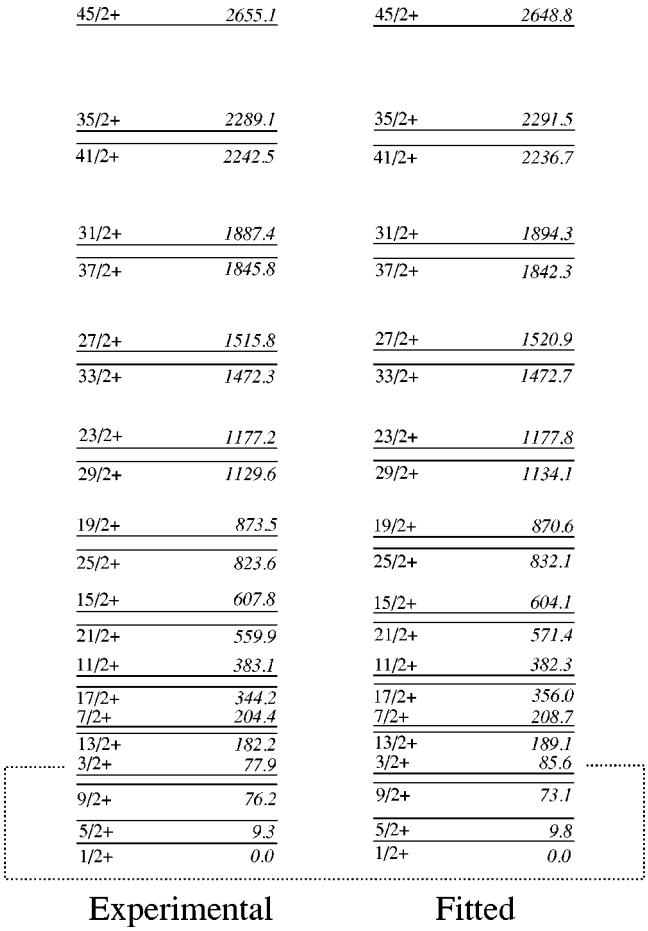

FIG. 11. A plot of experimental energies and fitted energies for the $K^{\pi}=1/2^{+}$ band using a minimization procedure to obtain best fit parameters to Eq. (2) for all the experimental levels shown. Levels within the dotted box are not drawn to scale.

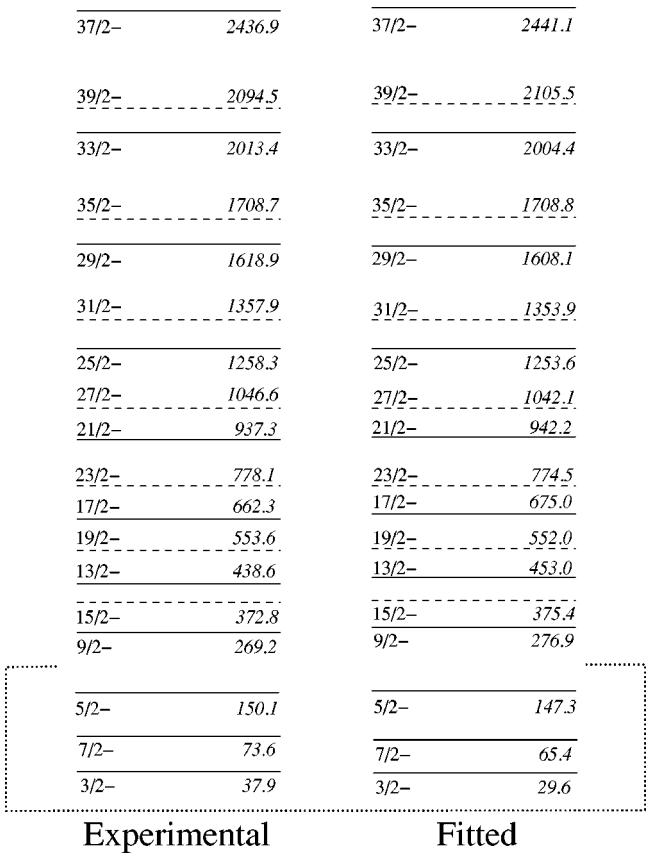

FIG. 12. A plot of experimental energies and fitted energies for the $K^{\pi}=1/2^{-}$ band using a minimization procedure to obtain best fit parameters to Eq. (2) for the experimental levels shown. An additional perturbation has been included into the fit for the levels of band 3, which are here denoted by dashed lines. For details of the parameters obtained see text. Levels within the dotted box are not drawn to scale.

The identification of $K^{\pi}=1/2^{\pm}$ bands allows the extraction of decoupling parameters which should provide a test of the proposed parity doublet nature. The decoupling parameter a can be obtained by fitting the experimental levels to Eq. (2). Liang *et al.* [12] performed calculations for ^{227}Th using a folded Yukawa reflection-asymmetric potential to predict values of the decoupling parameters in ^{227}Th. This strong coupling model approach (with $\varepsilon_3=0.08$) suggested $|a|=3$ for the $K^{\pi}=1/2$ bands. Such a value would lead to energetically degenerate levels that have J values differing by 3 in the favored and unfavored signatures of the $K=1/2$ bands (see Fig. 10). A cursory view of the proposed $K^{\pi}=1/2^{+}$ band shows a near degeneracy of this type, with the results of the fit (with the ground state fixed at zero) giving: $A=6.66$ keV, decoupling parameter $a=3.27$, $B=1.86\times10^{-3}$ keV, and $\varepsilon_K=20.16$ keV. The rms deviation of the fitted levels from experimental values is 4.7 keV and a comparison between fitted and experimental levels is shown in Fig. 11. It should be noted that any alternative spin ordering results in a very poor fit to the energy levels.

Unfortunately, applying a fit of the relationship given in Eq. (1) to the $K^{\pi}=1/2^{-}$ band results in a poor agreement between experimental and fitted energies. We have achieved a rather good fit, however, by assuming a fixed displacement of band 3 relative to the remainder of the $K^{\pi}=1/2^{-}$ band. This is incorporated into the fitting routine by fitting the levels of band 3 with a term ε_K' in place of ε_K, which is used for the remainder of the $K^{\pi}=1/2^{-}$ band. The term ε_K' is given by

$$\varepsilon_K'=\varepsilon_K+C, \tag{3}$$

where the constant C defines the displacement of band 3. The result of fitting all of the $K^{\pi}=1/2^{-}$ band gives: $A=5.92$ keV, decoupling parameter $a=-2.98$, $B=4.26\times10^{-4}$ keV, and $\varepsilon_K=45.64$ keV with $C=97.0$ keV. The rms deviation of the fitted levels from experimental values is 7.5 keV and a comparison between fitted and experimental levels is shown in Fig. 12. It should also be noted that the omission of the $J^{\pi}=39/2^{-}$ and $J^{\pi}=37/2^{-}$ levels from the fit results in a reduction of the rms deviation (to ≈6 keV) and could, therefore, indicate the presence of band crossing effects at the highest observed spins of the $K^{\pi}=1/2^{-}$ band. The decoupling parameters obtained for both $K^{\pi}=1/2^{+}$ and $K^{\pi}=1/2^{-}$ bands, $a=3.27$ and -2.98, respectively, lie close in magnitude with opposite sign. Such values suggest these

bands may be built upon a single intrinsic state of mixed parity. The agreement with the prediction of Liang *et al.* [12] ($|a|=3$) is also excellent. The nature of the perturbation, which generates the apparent displacement of the $K^\pi=1/2^-$ favored signature somewhere between $J^\pi=7/2^-$ and $J^\pi=15/2^-$, is unknown. Unfortunately we have not observed the expected $J^\pi=11/2^-$ level that might have thrown more light on the problem. As the band-mixing considerations of Liang *et al.* [12] in the intermediate coupling regime indicate considerable mixing between $K=1/2$ and $K=3/2$ states we have tested the hypothesis that Coriolis coupling between $K=1/2$ and $K=3/2$ bands could cause the perturbation. We have performed band-mixing calculations assuming a nonadiabatic Coriolis coupling between the $K^\pi=1/2^-$ and $K^\pi=3/2^-$ bands. These calculations are unable to generate the observed experimental levels and we can suggest no other satisfactory explanation for the perturbation of the $K^\pi=1/2^-$ band.

D. Parity splitting

The parity content of the intrinsic state can be estimated in the strong coupling limit from the parity splitting of the odd-A nucleus compared to that of the even-even neighbors [18],

$$\langle\hat{\pi}\rangle=\frac{E_{J^-}-E_{J^+}}{E(0^-)}, \tag{4}$$

where $\langle\hat{\pi}\rangle$ is the parity content of the intrinsic state in the odd-A nucleus, $E_{J^-}-E_{J^+}$ is the parity splitting of the nucleus concerned, and $E(0^-)$ is the splitting of the core, which can be approximated from the average of the extrapolated 0^- state in the nearest even-even neighbors. A parity content near unity suggests an intrinsic state of definite parity whereas a value near zero suggests an equal admixture of positive and negative parities in the intrinsic state. We use a value for the core splitting $E(0^-)=263$ keV obtained from the energies of the $J^\pi=1^-$ states in ^{226}Th and ^{228}Th [20] minus $\hbar^2/\mathcal{J}$.

We can also estimate the parity splitting between $K^\pi=1/2^\pm$ bands. First, the energy splitting between the intrinsic parity doublet can be approximated as the difference between the respective ε_K values for $K^\pi=1/2^\pm$ bands yielding a value of 25.5 keV. Alternatively the parity splitting can be calculated as a function of spin, independent of signature splitting, from the relationship [8]

$$\delta\hat{E}_\pi(J)=\frac{1}{2}[E_{s=+i}(J^-)-E_{s=+i}(J^+)+E_{s=-i}(J^-)-E_{s=-i}(J^+)], \tag{5}$$

where the levels are labeled by simplex and parity. In the calculation of $\delta\hat{E}_\pi(J)$, interpolation is used for spins with a forbidden combination of simplex and parity while in cases where neighboring levels have not been observed, extrapolation is performed over the two available neighbors of the same simplex. $\delta\hat{E}_\pi(J)$ is plotted as a function of spin in Fig. 13. The figure displays splitting calculated from the observed level energies as well as the hypothetical splitting obtained by subtracting the 97-keV offset of band 3 described in section *C*. The actual splitting (denoted in Fig. 13 by closed circles) displays a marked transition at the onset of band 3 as opposed to the hypothetical points (denoted in Fig. 13 by open circles) that continue along a smooth continuous curve. The parity splitting should indeed form a smooth continuous curve and, therefore, we take Fig. 13 as further evidence for the perturbation of band 3. From Fig. 13 we are able to give a limit for the parity content of the $K=1/2$ intrinsic state and find $0.0<\langle\hat{\pi}\rangle<0.2$. This value would seem to be in good agreement with the expectation of a parity doublet.

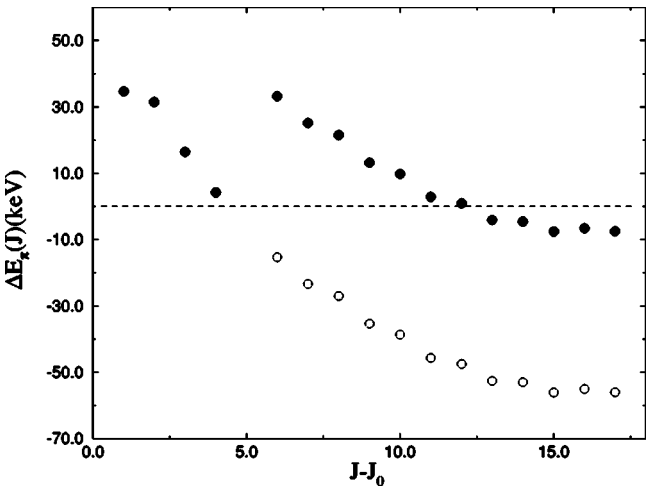

FIG. 13. The parity splitting of the $K^\pi=1/2^\pm$ doublet as a function of spin. Closed circles denote the experimental points while open circles denote the hypothetical splitting obtained by subtracting 97 keV from the experimental energy levels of band 3.

E. Electric dipole/quadrupole ratios

The determination of $B(E1)/B(E2)$ ratios for some of the transitions in ^{227}Th allows a comparison of the intrinsic D_0/Q_0 ratio with that of the neighboring even-even nuclei. According to Bohr and Mottelson [21], in the case of $K^\pi=1/2^+$ bands the spherical component of the intrinsic electric dipole moment is nonzero. The $E1$ transition strength can be written in terms of both D_0 and D_1 [22]

$$B(E1;J_i\rightarrow J_f)=\frac{3}{4\pi}\left|\langle J_iK_i10|J_fK_f\rangle D_0+(-1)^{[J_i+(1/2)]}\left\langle J_i-\frac{1}{2}11\middle|J_f\frac{1}{2}\right\rangle D_1\right|^2. \tag{6}$$

However, Bohr and Mottelson state that the experimental observations set an upper limit of 0.1 for the ratio D_1/D_0 and a more recent experimental investigation on the $B(E1)$ strengths between $K^\pi=1/2^+$ bands in ^{225}Ra concluded $D_1/D_0=0.07$ [23]. Similarly, D_1/D_0 ratios have been measured in ^{231}Th [24] and found to be <0.04. As these values are of the same order as the experimental errors associated

TABLE V. D_0/Q_0 ratios from measured $I_\gamma(E1)/I_\gamma(E2)$ values. The first five values given are for band 4 and the last value is for band 3. Further details on the calculation of these ratios is given in the text.

Gating transition (keV)	$E_\gamma(E1)$	$E_\gamma(E2)$	$D_0/Q_0(10^{-4}$ fm$^{-1})$
224.7 ($E2$)	113.9	178.7	2.37(9)
233.7 ($E1$)	113.9	178.7	2.4(1)
303.7 ($E2$)	211.2	265.7	2.5(2)
338.6 ($E2$)	239.8	303.7	2.7(3)
325.2 ($E1$)	239.8	303.7	2.5(4)
311.3 ($E2$)	223.0	268.5	2.8(3)

with our $B(E1)/B(E2)$ ratios, we ignore the contribution of D_1 to the $B(E1)$ strength and use the following relationships to obtain D_0/Q_0 ratios:

$$B(E1;J_i\rightarrow J_f)=\frac{3}{4\pi}\langle J_iK_i10|J_fK_f\rangle^2D_0^2, \tag{7}$$

$$B(E2;J_i\rightarrow J_f)=\frac{5}{16\pi}\langle J_iK_i20|J_fK_f\rangle^2Q_0^2, \tag{8}$$

which yields,

$$\frac{D_0}{Q_0}=\left(\frac{5}{16}\frac{B[E1,J\rightarrow(J-1)]}{B[E2,J\rightarrow(J-2)]}\frac{(J-K-1)(J+K-1)}{(J-1/2)(J-1)}\right)^{1/2}. \tag{9}$$

The deduced spin assignments allow the first accurate determination of D_0/Q_0 ratios for ^{227}Th. The values are given in Table V. Five values are given for band 4 (i.e., the $E2$ transitions in the $K^\pi=1/2^+$ band and the $E1$ transitions from the $K^\pi=1/2^+$ band to the $K^\pi=1/2^-$ band) and a further value is calculated for band 3 (i.e., the $E2$ transitions in the $K^\pi=1/2^-$ band and the $E1$ transitions from the $K^\pi=1/2^-$ band to the $K^\pi=1/2^+$ band). Taking the mean of the D_0/Q_0 ratios for the two neighboring even-even nuclei [25], we obtain a value of $\approx 2.6(10^{-3}$ fm$^{-1})$ against which the ratios of Table V can be compared. The agreement is excellent, suggesting that the strength of the octupole correlations for this particular neutron configuration in ^{227}Th is comparable with ^{226}Th and ^{228}Th. For a more direct systematic comparison of the electric dipole moment we can estimate Q_0 to be the mean of the values found experimentally for the two even-even neighbors. Assuming a 10% uncertainty from this procedure we obtain $|D_0|=0.21(3)e$ fm. In Fig. 14 we plot $|D_0|$ against N for the thorium isotopes (from $N=130$ to $N=140$). A smooth systematic trend is observed.

F. Miscellaneous levels

One last level of interest is a 24.3-keV $J^\pi=3/2^+$ state identified in previous studies of this nucleus [12,13] but not included in our level scheme. This spin and parity have been unambiguously assigned from a measured $M1$ transition to the ground state and this state has, therefore, been interpreted as the bandhead of a $K^\pi=3/2^+$ band. Furthermore, a γ ray of 51.9 keV observed in ^{231}U α-decay studies [13] has been proposed for a transition from a 76.2-keV level to the 24.3-keV level, which would limit that 76.2-keV level to $J\leqslant 7/2$ as opposed to our assignment of $J=9/2$. Manns *et al.* suggested that band 1, linked via the 51.9-keV transition, has $K^\pi=3/2^+$. This arrangement leads to inherent problems with the spin assignments of the low-lying structure. Therefore, although we agree that the 24.3-keV level is a strong candidate for a $K^\pi=3/2^+$ bandhead, we believe the 51.9-keV γ ray observed by Müller *et al.* [13] is unlikely to originate from the 76.2-keV state observed in the present work. We feel this transition is more likely to originate from another almost degenerate level, such as the unobserved $K^\pi=1/2^-$, $J^\pi=1/2^-$ state that is expected at an energy close to 76 keV. It is perhaps also worth noting that the 24.3-keV ($3/2^+$) level is linked to the 99.2-keV level [13], which is possibly the $5/2^+$ member of the $K^\pi=3/2^+$ band although we have been unable to locate any candidate for higher members of this band. As we cannot determine whether this $K^\pi=3/2^+$ band forms a parity doublet with the $K^\pi=3/2^-$ band it is not possible to deduce whether the $K^\pi=3/2^-$ band describes reflection-symmetric or reflection-asymmetric collective excitation.

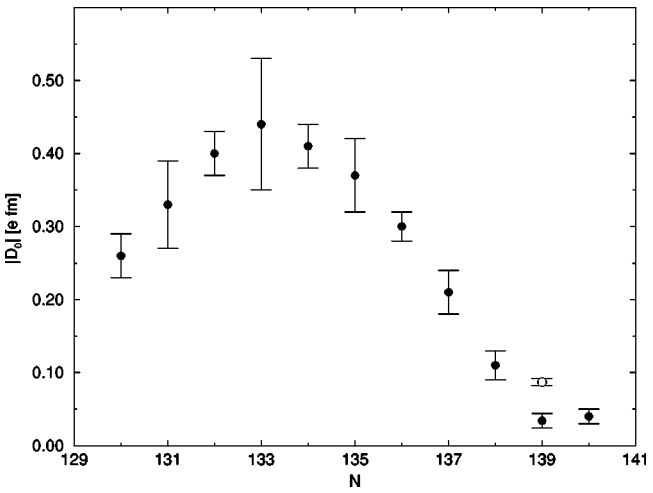

FIG. 14. A plot of electric dipole systematics for thorium isotopes. Closed circles represent measured dipole moments in the ground state band. The second point given for ^{229}Th and denoted by an open circle is the measured dipole moment in an excited $K=3/2^\pm$ parity doublet band. Data is taken from [8,9,20,26].

IV. CONCLUSION

The level structure of ^{227}Th has been studied in the ^{226}Ra(α,3n)^{227}Th reaction at a bombarding energy of 33 MeV. Previously observed high-spin rotational sequences have been confirmed and extended to higher and lower excitation energies. The relative positions of these sequences have been refined, allowing the successful inclusion of the larger number of high-spin states into the low-spin decay structure for the first time. The level structure is described by Coriolis staggered $K^\pi=1/2^\pm$ parity doublet bands and a $K^\pi=3/2^-$ sequence with a further tentatively assigned band deduced from interband transitions. The remarkable four pa-

rameter fit to the 21 levels of the $K^\pi=1/2^+$ band provides further strong confirmation, if needed, of the $J^\pi=1/2^+$ assignment to the ground state of ^{227}Th. The favored signature of the $K^\pi=1/2^-$ band appears to become perturbed between the $J^\pi=7/2^-$ and $J^\pi=15/2^-$ levels. The interaction responsible for this effect is unknown. Coriolis coupling to the $K^\pi=3/2^-$ band does not appear to be a likely source of the perturbation based upon our band-mixing calculations. Instead, the levels appear to have been displaced in energy by a constant 97.0-keV offset, a reduction of this amount from the energies of the perturbed levels allows a convincing fit of the whole $K^\pi=1/2^-$ band to the relationship given in Eq. (1). $K^\pi=1/2^\pm$ bands have decoupling parameters that are of similar absolute values but different signs as expected for a reflection-asymmetric rotor. The magnitude of the decoupling parameters is also close to that predicted by Liang *et al*. within the strong coupling basis. These bands form a parity doublet and ^{227}Th is, therefore, shown to exhibit considerable octupole deformation in the ground state configuration. This interpretation is further strengthened by an estimation of the parity content of the $K=1/2$ intrinsic state. Consideration of parity splitting in the $K^\pi=1/2^\pm$ bands gives a parity content that is positive with an upper limit of 0.2. This is approaching the value of zero expected for an intrinsic state of equally mixed positive and negative parities. D_0/Q_0 ratios for the $K^\pi=1/2^\pm$ bands have been calculated from measured $B(E1)/B(E2)$ values and were found to be consistent with the mean value of the D_0/Q_0 ratios given for neighboring even-even nuclei. This result provides further evidence of strong octupole collectivity.

ACKNOWLEDGMENTS

This work was supported by the U.K. Engineering and Physical Sciences Research Council, the European Union Fifth Framework Programme ''Improving Human Potential—Access to Research Infrastructure'' (Contract No. HPRI-CT-1999-00044), and by the the Academy of Finland under the Finnish Centre of Excellence Programme 2000–2005 (Project No. 44875, Nuclear and Condensed Matter Physics Programme at JYFL). N.J.H. and R.D.H. would like to thank the EPSRC for financial support. The EUROGAM detectors were provided from the U.K./France EPSRC/IN2P3 loan pool. The NORDBALL detectors were provided by the Niels Bohr Institute, Denmark.

[1] K. Alder, A. Bohr, T. Huus, B. Mottelson, and A. Winther, Rev. Mod. Phys. **28**, 432 (1956).
[2] K. Lee and D.R. Inglis, Phys. Rev. **108**, 774 (1957).
[3] I. Ahmad and P.A. Butler, Annu. Rev. Nucl. Part. Sci. **43**, 71 (1993).
[4] P.A. Butler and W. Nazarewicz, Rev. Mod. Phys. **68**, 349 (1996).
[5] R.R. Chasman, Phys. Lett. **96B**, 7 (1980).
[6] S. Ćwiok and W. Nazarewicz, Phys. Lett. B **224**, 5 (1989).
[7] S. Ćwiok and W. Nazarewicz, Nucl. Phys. **A529**, 95 (1991).
[8] M. Dahlinger, E. Kankeleit, D. Habs, D. Schwalm, B. Schwartz, R.S. Simon, J.D. Burrows, and P.A. Butler, Nucl. Phys. **A484**, 337 (1988).
[9] J.R. Hughes, R. Tölle, J. De Boer, P.A. Butler, C. Günther, V. Grafen, N. Gollwitzer, V.E. Holliday, G.D. Jones, C. Lauterbach, M. Marten-Tölle, S.M. Mullins, R.J. Poynter, R.S. Simon, N. Singh, R.J. Tanner, R. Wadsworth, D.L. Watson, and C.A. White, Nucl. Phys. **A512**, 275 (1990).
[10] G.I. Novikova, E.A. Volkova, L.I. Goldin, D.D. Ziv, and E.F. Tretyakov, Zh. Eksp. Teor. Fiz. **37**, 928 (1960) [Sov. Phys. JETP **10**, 663 (1960)].
[11] C.F. Liang, R.K. Sheline, P. Paris, M. Hussonnois, J.F. Ledu, and D.B. Isabelle, Phys. Rev. C **49**, 2230 (1994).
[12] C.F. Liang, P. Paris, R.K. Sheline, D. Nosek, and J. Kvasil, Phys. Rev. C **51**, 1199 (1995).
[13] U. Müller, P. Sevenich, K. Freitag, C. Günther, P. Herzog, G.D. Jones, C. Kliem, J. Manns, T. Weber, and B. Will, ISOLDE Collaboration, Phys. Rev. C **55**, 2267 (1997).
[14] J. Manns, J. Gröger, C. Günther, U. Müller, T. Weber, and J. de Boer, Eur. Phys. J. A **3**, 263 (1998).
[15] P.J. Nolan, Nucl. Phys. **A520**, 657c (1990).
[16] P.J. Nolan, D.W. Gifford, and P.J. Twin, Nucl. Instrum. Methods Phys. Res. A **236**, 95 (1985).
[17] B. Herskind, in *Proceedings of the Second International Conference on Nucleus Nucleus Collisions*, edited by H. Å. Gustafsson, B. Jakobsson, I. Otterlund, and K. Alekett [Nucl. Phys. **A447**, 395c (1986)].
[18] G.A. Leander and Y.S. Chen, Phys. Rev. C **37**, 2744 (1988).
[19] G.D. Jones, T.H. Hoare, P.A. Butler, and C.A. White, J. Phys. G **17**, 713 (1991); T. H. Hoare, Ph.D. thesis, University of Liverpool, 1991; G.D. Jones, P.A. Butler, T.H. Hoare, and P.M. Jones, Eur. Phys. J. A **2**, 129 (1998).
[20] P. Schüler, Ch. Lauterbach, Y.K. Agarwal, J. De Boer, K.P. Blume, P.A. Butler, K. Euler, Ch. Fleischmann, C. Günther, E. Hauber, H.J. Maier, M. Marten-Tölle, Ch. Schandera, R.S. Simon, R. Tölle, and P. Zeyen, Phys. Lett. B **174**, 241 (1986).
[21] A. Bohr and B. R. Mottelson, *Nuclear Structure* (Benjamin, New York, 1975), Vol. 2.
[22] P.A. Butler and W. Nazarewicz, Nucl. Phys. **A533**, 249 (1991).
[23] C.W. Reich, I. Ahmad, and G.A. Leander, Phys. Lett. **169B**, 148 (1986).
[24] A.J. Aas, H. Mach, J. Kvasil, M.J.G. Borge, B. Fogelberg, I.S. Grant, K. Gulda, E. Hagebø, P. Hoff, W. Kurcewicz, A. Lindroth, G. Løvhøiden, A. Mackova, T. Martinez, B. Rubio, M. Sánchez-Vega, J.F. Smith, J.L. Tain, R.B.E. Taylor, O. Tengblad, and T.F. Thorsteinsen, ISOLDE Collaboration, Nucl. Phys. **A654**, 499 (1999).
[25] B. Ackermann, H. Baltzer, C. Ensel, K. Freitag, V. Grafen, C. Günther, P. Herzog, J. Manns, M. Marten-Tölle, U. Müller, J. Prinz, I. Romanski, R. Tölle, J. deBoer, N. Gollwitzer, and H.J.

Maier, Nucl. Phys. **A559**, 61 (1993).
[26] K. Gulda, W. Kurcewicz, A. J. Aas, M. J. G. Borge, D. G. Burke, B. Fogelberg, I. S. Grant, E. Hagebø, N. Kaffrell, J. Kvasil, G. Løvhøiden, H. Mach, A. Mackova, T. Martinez, G. Nyman, B. Rubio, J. L. Tain, O. Tengblad, and T. F. Thorsteinsen, Nucl. Phys. (to be published).
[27] R.S. Hager and E.C. Seltzer, Nucl. Data, Sect. A **4**, 1 (1968).